Centrum voor Wiskunde en Informatica
**REPORT***RAPPORT*

# Revealing Local Variability Properties of Human Heartbeat Intervals with the Local Effective H¦lder Exponent

Z.R. Struzik

Information Systems (INS)

**INS-R0015 June 30, 2000**

Report INS-R0015
ISSN 1386-3681

CWI
P.O. Box 94079
1090 GB Amsterdam
The Netherlands

# Revealing Local Variability Properties of Human Heartbeat Intervals with the Local Effective Hölder Exponent

Zbigniew R. Struzik
*CWI*
*P.O. Box 94079, 1090 GB Amsterdam, The Netherlands*
*email:* Zbigniew.Struzik@cwi.nl

ABSTRACT
The local effective Hölder exponent has been applied to evaluate the variability of heart rate locally at an arbitrary position (time) and resolution (scale). The local effective Hölder exponent [8, 9] used is effectively insensitive to local polynomial trends in heartbeat rate due to the use of the Wavelet Transform Modulus Maxima technique. Also the variability so obtained is compatible in the sense of distribution to the Multifractal Spectra of the analysed heart rate time series. This provides the possibility of standardising the variability estimation for comparison between different patients and between different recordings for one patient. The previously reported global correlation behaviour [1] is captured in the effective Hölder exponent based, local variability estimate. This includes discriminating healthy and sick (congestive heart failure patients) on the basis of both the central (Hurst) exponent and the width of the multifractal spectra. In addition to this, we observed intriguing patterns of individual response in variability records to daily activities. A moving average filtering of Hölder exponent based variability estimates was used to enhance these fluctuations. We find that this way of local presentation of scaling properties may be of clinical importance.

*2000 Mathematics Subject Classification:* 28A80, 65Z05, 68T10, 68P10
*1998 ACM Computing Classification System:* H1, I5, Jm, J2, E2
*Keywords and Phrases:* multifractal analysis, wavelet transform, Hölder exponent, local scaling, heartbeat variability
*Note:* full colour version of this paper can be downloaded from www.cwi.nl/~zbyszek

## 1. Introduction

Recent findings reported in [1] suggest that heartbeat rate is more complex than has been anticipated, requiring multiple, densely interwoven scaling (roughness) exponents to describe it. This is in contrast to the more established view which associated one global roughness exponent with each heartbeat record [2]. This exponent, of course, could be different for various people and also depended on the state of health. A multifractal description reveals exponents changing from point to point in a way which suggests some higher order organisation. Such multifractal exponents cannot be simply grouped in patches of constant or stationary behaviour, but display complex, non-stationary structure at any time scale (resolution) considered.

The multifractality discovery was possible thanks to the application of the wavelet transform (modulus maxima) method to perform the multifractal analysis of the heartbeat signal. The formalism, developed by Arneodo et al in the early nineties has been successfully used to test many natural phenomena [3, 4, 5, 6, 7]. One of the key aspects of this methodology is, however, that it is intrinsically statistical and provides only *global* estimates of scaling (of the moments of relevant quantity). While this is often a required property, in some cases local information about scaling might provide more relevant information than the global spectrum. This is particularly true for time series where scaling properties are non-stationary, whether it be due to intrinsic changes in the signal scaling characteristics, noise or simply the boundary effects.

To address this problem, we have introduced [8, 9] a method of estimation of the *local* scaling exponent through the paradigm of the multiplicative cascade. We reveal the hierarchy of the scaling branches of the cascade with the wavelet transform modulus maxima tree, which has proved to be an excellent tool for the purpose [4, 10]. Contrary to the intrinsically instable local slope of the maxima lines, this estimate is robust and provides a stable, effective Hölder exponent, local in scale and position.

For model multifractals, the mechanism behind multiscale non-stationarity in the roughness exponent values does not change with resolution (scale). It can be captured in a distribution (or spectrum) of multifractal exponents, which for idealised multifractal signals shows the same spectrum independent of the length or starting position of the investigated time series. Such behaviour is typical for model multifractals, but in heartbeat and in other real life signals, changes are observed in all spectral characteristics: positioning, shape and modality, depending on the time series investigated, but also on the selected time and scale range of analysis.

While this adds to the complexity of the global (spectral) description, it also validates the local approach, where we choose to look back at the temporal organisation of the scaling (effective Hölder) exponent in the hope that the analysis of its intrinsic non-stationarities will provide insight into global behaviour. [1]

In this paper, we applied the local effective Hölder exponent to evaluate the variability of the heartbeat rate locally at an arbitrary position (time) and resolution (scale). Just as is the case in global Wavelet Transform Modulus Maxima based Multifractal Formalism, the technique is effectively insensitive to local polynomial trends in heartbeat rate. Also the variability so obtained is compatible in the sense of distribution to the multifractal spectra of the analysed heartbeat rate time series.

Therefore, the previously reported global correlation behaviour is captured in the effective Hölder exponent based, local variability estimate. This includes discriminating healthy and sick (congestive heart failure patients) on the basis of both the central (Hurst) exponent [2] and the width of the multifractal spectra [1]. However, in addition to this, we observed intriguing patterns of individual response (non-stationarities) in variability records to daily activities and during sleep.

The observation of non-stationarity of the variability estimate obtained with the effective Hölder exponent prompted us to conduct a series of experiments. The main objective of the tests was to develop a methodology capable of answering of the following questions:

1. Is the observed multifractal behaviour of the heartbeat the result of non-stationarity of the local effective Hölder exponent?

2. Can the non-stationarity be linked with activity, i.e. the particular mental or somatic state of the person?

3. In the case of known physiological input like beta-blocker, is the non-stationarity still observed?

4. In the case of non-activity such as during sleep, is the non-stationarity still observed?

Of course all the above questions lead to the central question of the physiological reasons for the apparent multifractal behaviour of the heartbeat. We will not attempt to give answer to this in this mainly methodological paper. Rather we will show that the methods described can give answers to particular questions of the kind listed above. We, therefore, hope that the methodology presented can help, through extensive study, in understanding systems characterised by apparently multifractal behaviour.

The structure of the paper is as follows. In section 2, we focus on the relevant aspects of the wavelet transformation, in particular the ability to characterise scale-free behaviour through the Hölder exponent. Together with the hierarchical, scale-wise decomposition provided by the wavelet transform, it will enable us to reveal the scaling properties of the tree of the multiplicative cascading process. In

[1] for example, into the way the spectrum is built.

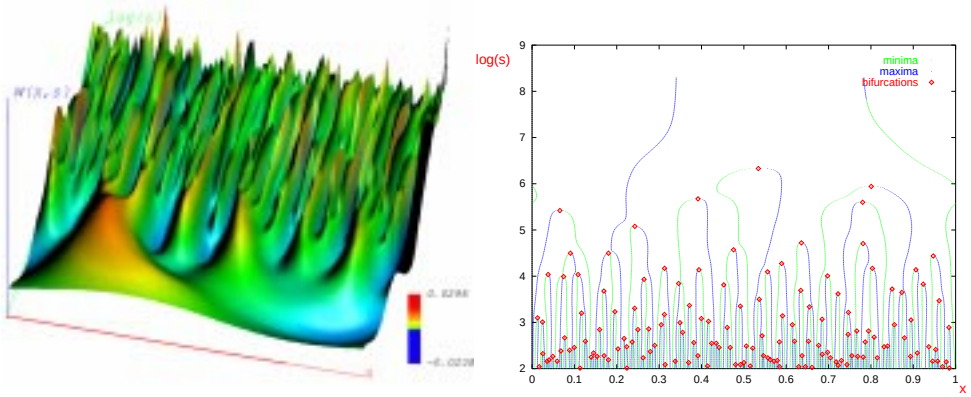


Figure 1: Left: Continuous Wavelet Transform representation of the random walk (Brownian process) time series. The wavelet used is the Mexican hat - the second derivative of the Gaussian kernel. The coordinate axes are: position $x$, scale in logarithm $\log(s)$, and the value of the transform $W(s,x)$. Right: The related WTMM representation.

section 3, we briefly describe a technical model enabling us to estimate the scale-free characteristic (the effective Hölder exponent) for the branches of such a process. A more extensive coverage of this method is available in [8, 9]. In section 4, we use the derived effective Hölder exponent for the local temporal description of the various test heartbeat time series. Section 5 provides an extension to fluctuation analysis of the effective Hölder exponent. Again a number of test signals are used to illustrate the effectiveness of the method and address the central questions arising from the non-stationarity of local effective Hölder exponent. Section 6 closes the paper with conclusions.

## 2. Continuous Wavelet Transform and its Maxima Used to Reveal the Structure of Singularities in the Time Series

Conceptually, the wavelet transformation [11, 12] is a convolution product of the time series with the scaled and translated kernel - the wavelet $\psi(x)$, usually a $n-th$ derivative of a smoothing kernel $\theta(x)$. Usually, in the absence of other criteria, the preferred choice is the kernel, since it is well localised both in frequency and position. In this paper, we chose the Gaussian $\theta(x) = \exp(-x^2/2)$ as the smoothing kernel, which has optimal localisation in both domains.

The scaling and translation actions are performed by two parameters; the scale parameter $s$ 'adapts' the width of the wavelet kernel to the resolution required and the location of the analysing wavelet is determined by the parameter $b$:

$$Wf(s,b) = \frac{1}{s} \int_{-\infty}^{\infty} dx\ f(x)\ \psi(\frac{x-b}{s})\ ,$$

where $s, b \in \mathbf{R}$ and $s > 0$ for the continuous version (CWT).

The 3D plot in figure 1 shows how the wavelet transform reveals more and more detail while going towards smaller scales, i.e. towards smaller $\log(s)$ values. The wavelet transform is sometimes referred to as the 'mathematical microscope' [4], due to its ability to focus on weak transients and singularities in the time series. The wavelet used determines the optics of the microscope; its magnification varies with the scale factor $s$.

This property makes the continuous wavelet transform very useful in analysing local regularity (scaling/roughness) properties of functions. In particular, such local scaling behaviour is often characterised by the Hölder exponent $h$. The following scaling equation defines the Hölder exponent $h(x_0) \in (n, n+1)$ of the cusp singularity at $x_0$:

$$|f(x) - P_n(x - x_0| \leq C|x - x_0|^h \ , \tag{2.1}$$

as the supremum of all $h$ such that the above relation holds for some polynomial $P_n$ of degree $n < h$. $P_n$ can often be associated with the Taylor expansion of $f$ around $x_0$, but Eq. 2.1 is valid even if such an expansion does not exist [15]. The Hölder exponent is, therefore, a function defined for each point of $f$, and it describes the local regularity of the function (or distribution) $f$.

It can be shown [13] that for cusp singularities, the location of the singularity can be detected, and the related exponent can be recovered from the scaling of the Wavelet Transform, along the so-called *maxima line*, converging towards the singularity. This is a line where the wavelet transform reaches local maximum (with respect to the position coordinate). Connecting such local maxima within the continuous wavelet transform 'landscape' gives rise to the entire tree of maxima lines. Restricting oneself to the collection of such maxima lines provides a particularly useful representation [14] of the entire CWT, the so-called Wavelet Transform Modulus Maxima representation (WTMM). It incorporates the main characteristics of the WT: the ability to reveal the *hierarchy* of (singular) features, including the scaling behaviour. In particular, we have the following power law proportionality for the wavelet transform of the cusp singularity in $f(x_0)$:

$$W^{(n)}f(s, x_0) \sim |s|^{h(x_0)} \ .$$

This is under the condition that the wavelet has at least $n$ vanishing moments, i.e. it is orthogonal to polynomials up to degree $n$: $\int_{-\infty}^{+\infty} x^m \, \psi(x) \, dx = 0 \quad \forall m, \ 0 \leq m < n$ . The reader will note that this requirement is needed to filter the polynomial $P_n$ in Eq. 2.1 in order to access the unbiased scaling exponent.

## 3. Estimation of the Local, Effective Hölder Exponent Using the Multiplicative Cascade Model

We have shown in the previous section that the wavelet transform, and in particular its maxima lines, can be used in evaluating the Hölder exponent in isolated singularities. In most real life situations, however, the singularities in the time series are not isolated but densely packed. The logarithmic rate of increase or decay of the corresponding wavelet transform maximum line is usually not stable but fluctuates, following the action of some process involved.

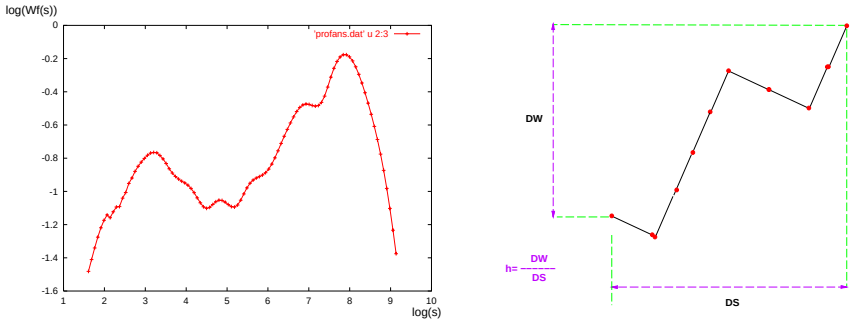


Figure 2: Left: It is impossible to evaluate the scaling exponent for an arbitrary maximum line participating in a complex process: a real life example of a maximum line. Right: The local effective Hölder exponent estimate takes the effective difference in the logarithm of the density of the process with respect to the logarithm of the scale difference gained along the process path.

To capture the fluctuations and estimate the related exponents (to which we will refer to as an *effective* [8] Hölder exponent of the singularity), we will model the singularities as created in some

kind of a collective process of a very generic class - the multiplicative cascade model. Each point of this cascade is uniquely characterised by the sequence of indices $(s_1 ... s_n)$, taking index values from the set of weights $\{p_i\}$. The sequence indicates the unique order in which the weights are successively acting along the process branch leading to the particular singularity.

Suppose that we denote the density of the cascade at the generation level $F_i$ ($i$ running from 0 to $max$) by $\kappa(F_i)$, we then have

$$\kappa(F_{max}) = p_{s_1} \ldots p_{s_n} \; \kappa(F_0) = P_{F_0}^{F_{max}} \; \kappa(F_0)$$

and the local exponent is related to the rate of increase of the product $P_{F_0}^{F_{max}}$ over the gained scale difference. In any experimental situation, the weights $p_i$ are not known and $h$ has to be estimated. This can be simply done using the fact that for the multiplicative cascade process, the effective product of the weighting factors is reflected in the difference of logarithmic values of the densities at $F_0$ and $F_{max}$ along the process branch:

$$h_{F_{max}}^{F_0} = \frac{\log(\kappa(F_{max})) - \log(\kappa(F_0))}{\log((1/2)^{max}) - \log((1/2)^0)} \; .$$

The densities along the process branch can be estimated with the wavelet transform, using its remarkable ability to reveal the entire process tree of a multiplicative process [10]. It can be shown that the densities $\kappa(F_i)$ correspond with the value of the wavelet transform along the maxima lines belonging to the given process branch. The estimate of the effective Hölder exponent becomes:

$$\hat{h}_{s_{lo}}^{s_{hi}} = \frac{\log(Wf\omega_{pb}(s_{lo})) - \log(Wf\omega_{pb}(s_{hi}))}{\log(s_{lo}) - \log(s_{hi})} \; ,$$

where $Wf\omega_{pb}(s)$ is the value of the wavelet transform at the scale $s$, along the maximum line $\omega_{pb}$ corresponding to the given process branch $bp$. Scale $s_{lo}$ corresponds with generation $F_{max}$, while $s_{hi}$ corresponds with generation $F_0$, (simply the largest available scale in our case). [2]

## 4. Employing the Local Effective Hölder Exponent in the Characterisation of Heartbeat Interval Time Series

Such an estimated local $\hat{h}(x_0, s)$ can be depicted in a temporal fashion, for example with colour stripes as we have done in figure 3. The colour of the stripes is determined by the value of the exponent $\hat{h}(x_0, s)$ and its location is simply the $x_0$ location of the analysed singularity (in practice this amounts to the location of the corresponding maximum line). Colour coding is done with respect to the mean value, which is set to the green colour central to our rainbow range. All exponent values lower than the mean value are given colours from the 'warmer' side of the rainbow, all the way towards dark red. All higher than average exponents get 'colder' colours, down to dark blue.

The first example in figure 3 is a record [17] of heartbeat intervals recorded from a healthy human heart and it shows an intricate structure of interwoven singularities at various strengths. This behaviour has been recently reported [1] to correspond with the multifractal behaviour of the heartbeat. The green is centred at $\hat{h} = 0.1$ for this panel. The second example time series is a computer generated sample of white noise. It shows almost monochromatic behaviour, centred at $h = -0.5$. The colour green is dominant. There are, however, several instances of darker green and light blue, indicating locally smooth components.

To the right of figure 3, the log-histograms are shown of the Hölder exponent displayed in the colour panels. They are made by taking the logarithm of the measure in each histogram bin. This conserves

[2] For $s_{lo}$ we will use $a = 5$ in the examples presented in this report. This is the lowest resolution for which we can maintain the shape of the Mexican hat.

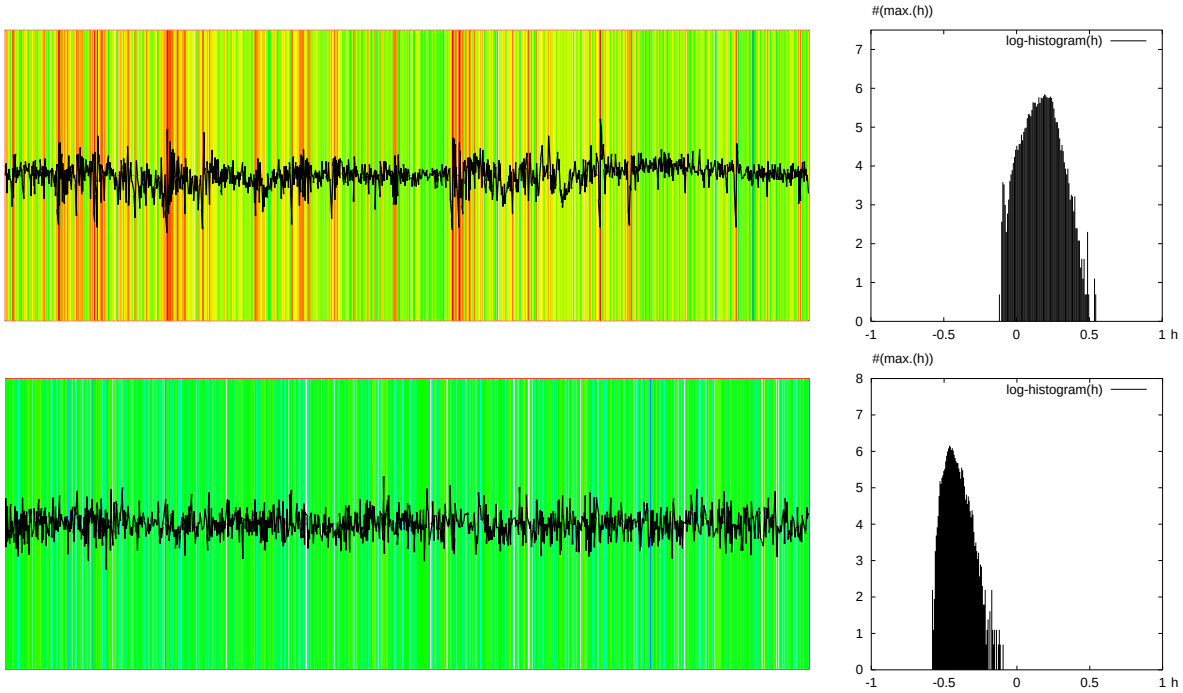


Figure 3: Left: Example time series with local Hurst exponent indicated in colour: the record of healthy heartbeat intervals and white noise. The background colour indicates the Hölder exponent locally, centred at the Hurst exponent at green; the colour goes towards blue for higher $\hat{h}$ and towards red for lower $\hat{h}$. Right: The corresponding log-histograms of the local Hölder exponent. (For colour version of this figure, see note on the first page of this report.)

the monotonicity of the original histogram, but allows us to compare the log-histograms with the spectrum of singularities $D(h)$. The log-histograms are actually closely related to the (multifractal) spectra of the Hölder exponent [9]. The multifractal spectrum of the Hölder exponent is the 'limit histogram' $D_{s\to 0}(h)$ of the Hölder exponent in the limit of infinite resolution. Of course we cannot speak of such a limit other than theoretically and, therefore, a limit histogram (multifractal spectrum) has to be estimated from the evolution of the log-histograms along scale. For details see [9].

The ability to display the scaling properties of the time series in a local manner has already proven quite successful. We have applied the method to a set of heartbeat interval time series in a (double) blind test. The purpose of the test was to establish whether the local effective Hölder exponent 'panels' can be used in discerning whether the time series is from a healthy or an ill subject.

In figure 4, we show one such set of panels. There are two records of healthy heartbeats and two of heart disease. The centre value of the effective Hölder exponent is $h = 0.1$, and is displayed in green colour. For $h > 0.1$ the colour becomes darker green, through light blue, it saturates as dark blue for $h = 0.5$. All $h > 0.1$ correspond with a higher than average local degree of correlation, which has been associated with heart failure. On the contrary, all $h < 0.1$ indicate stronger than average (relative) anti-correlation, which can be associated with healthy heartbeat behaviour. The colours displayed for $h < 0.1$ are from light green through yellow and orange towards red at $h = -0.3$.

The two upper panels 1) and 2) in figure 4 both belong to healthy individuals but of course there is no reason why they should be identical. And indeed individual patterns all have a different arrangement of colour stripes. Also the density of colours changes; some non-stationary behaviour is apparent in the figures 4, panels 1) and 2). Both panels show a wide range of colours reflecting fully developed dynamics of the healthy heartbeat. Such panels correspond to a wide multifractal spectrum [1].

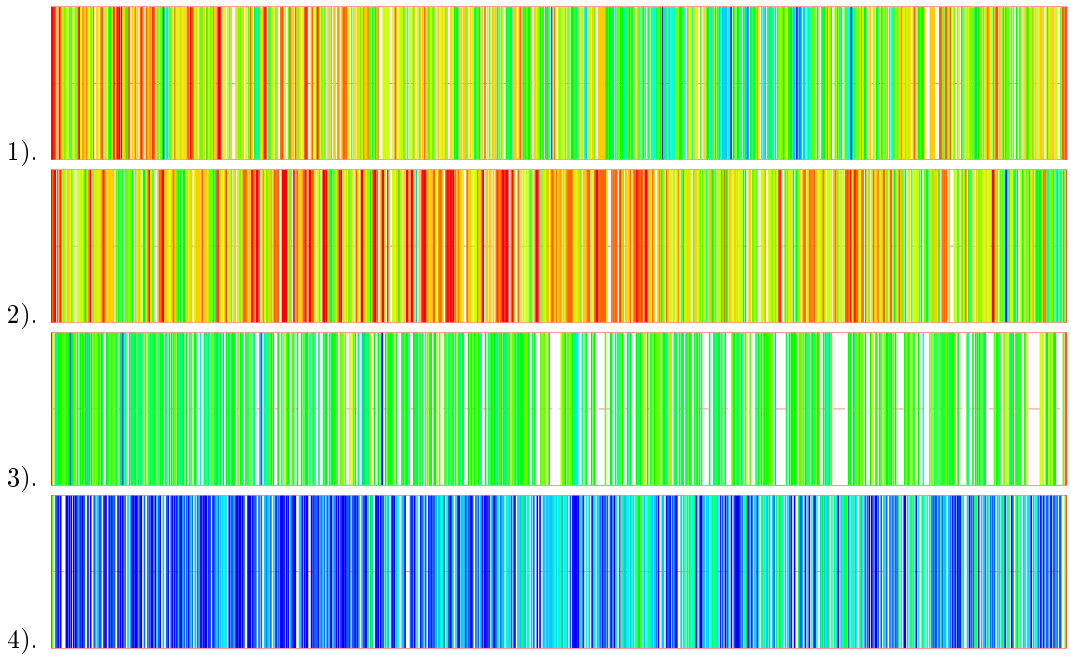


Figure 4: Local Hurst exponent indicated in colour for four heartbeat interval time series (not shown). The green colour is centred at $h = 0.0$ for all plots. It saturates at dark blue for $h = 0.4$ and at dark red for $h = -0.4$. (For colour version of this figure, see note on the first page of this report.)

The two lower panels 3) and 4), on the contrary, are taken from heartbeats of congestive heart failure (CHF) cases. The deviation from healthy behaviour can occur in a number of ways but these two are perhaps the most generic. One type of deviation causes a narrowing of the dynamics and therefore a narrowing of the range of colours - it is reminiscent of the monofractal noise shown in figure 3. The other type of deviation, in addition to a narrower colour spectrum, is that it drifted away in its entire colour spectrum in the direction of green and blue, that is smoother (more correlated) behaviour. This shift in the central colour reflects the change in the global correlation exponent between healthy and CHF individuals [2].

We have left the background between the stripes uncoloured (white) although it corresponds with even more smooth regions (at the resolution considered!) and can all be painted dark blue. This would enhance the colour range and help diagnosis, but we preferred not to introduce any additional information to the panels in this research paper.

It is apparent that the colour panels provide more information than the global averages, like the central colour or the range of colours used (i.e.- the width of the multifractal spectrum). In the following, we will show how to exploit this additional information pertinent to the local colour fluctuations (non-stationarities) in the panels.

## 5. Collective Properties of the Local Variability Estimate

In the context of heartbeat, one may ask the question: what is the meaning of the varying local scaling exponent. Also its temporal organisation and its relevance to the multifractal spectrum may be tested. Ultimately, we would like to identify physiological reasons for the apparent multifractal behaviour of the heartbeat. Let us first go back to numerical information, the Hölder exponent which we used to represent in colour, and exploit a few generic cases of non-stationarity.

In figure 5, three example heartbeat interval time series are shown with their corresponding local effective Hölder exponent. The first example from the left (bottom plot) shows a consistent linear

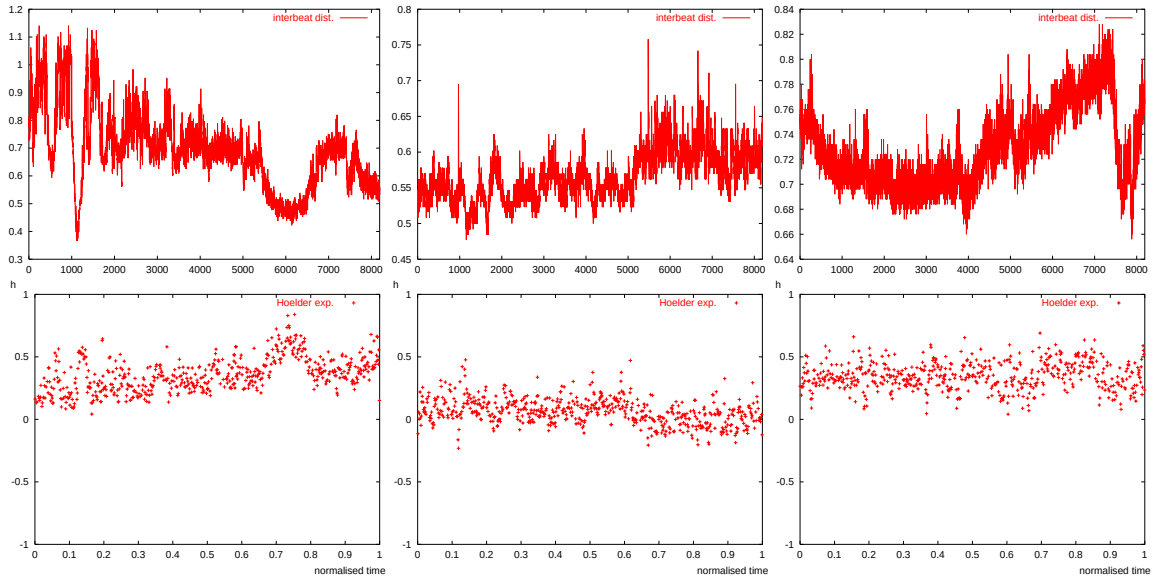


Figure 5: Three example heartbeat interval time series (top row) with their corresponding local effective Hölder exponent (bottom row). Two examples of non-stationarities in local Hölder exponent; they are intrinsic to the local Hölder exponent not to the non-stationarities of the input time series, as is shown in the third example, showing independence of the polynomial trend in the input.

trend - the increase of the exponent value with time. This can also be verified in the corresponding time series above (leftmost, top plot): the roughness of the time series decreases with time (except for some minor fluctuations). In the second example (centre panel), two distinct regimes can be distinguished with a somewhat different mean $h$ value: one region up until sample 5000 and the other of slightly lower value of $h$ for samples 5500 and more. Both the above cases will result in a broadening of the $D(h)$ spectrum as a result of the non-stationary behaviour of $h$. This effect alone, if observed at one global resolution, would not be sufficient for multifractal behaviour - it would simply mean that the local variability is non-stationary in these time series. In the following, we will detect multiscale non-stationarity of $h$. In the last example in the rightmost panels, we show that the $h$ exponent and the roughness of the time series are independent of the fluctuations or trends in the time series.

The evident non-stationary behaviour in these figures can be quantified, and for this purpose we used a low pass moving average filter (MA) to detect/enhance trends. This processing is, of course, done on the Hölder exponent value set $\{h_i(f(x))\}$, *not* on the input signal $f(x)$ . A $n$-MA filtering of $n$ base is defined as follows:

$$h_{MA_n}(i) = \frac{1}{n}\sum_{i=1}^{i=n} h_i(f(x)) \ , \tag{5.1}$$

where $h_i(f)$ are the subsequent values of the effective Hölder exponent of the time series $f$. Standard deviation from the $h_{MA_n}(i)$ mean exponent can also be calculated:

$$SDh_{MA_n}(i) = \frac{1}{n}\sqrt{\sum_{i=1}^{i=n}(h_i(f(x)) - h_{MA_n}(i))^2} \ . \tag{5.2}$$

The observation of non-stationarity of the variability estimate obtained with the effective Hölder

exponent prompted us to do a series of experiments. The main objective of the test was to attempt to answer the questions posed in the Introduction. In the following, we are going to show how the techniques described can help in finding the answers to those questions. We analysed several data sets but only the typical behaviour will be presented, leaving broader coverage of the data and related conclusions to a separate publication.

As already indicated above, even though the fluctuations in the heart rate variability are clearly visible in the effective Hölder exponent data, they will benefit from filtering with the moving average filter. The moving average, Eq. 5.1 is performed directly on the subsequent ordered maxima, each carrying the corresponding effective Hölder exponent value. The number of maxima at the lowest scale of analysis is only roughly related to the number of heartbeats in the time series. However, this problem is negligible for the large length of averaged exponent values (we use 100, 1000, 10000 exponent values, i.e. maxima lines). Since the actual temporal information can be associated with each maximum value, we map it back on the average values obtained from the moving average and use it for the abscissa of the plots. Additionally, for each moving average window, we calculate the standard deviation from the mean value. This standard deviation, Eq. 5.2 is closely related to the width of histograms of the local effective Hölder exponent. Therefore it also reflects the width of the multifractal spectra over $MA$-base, the range of the moving average window.

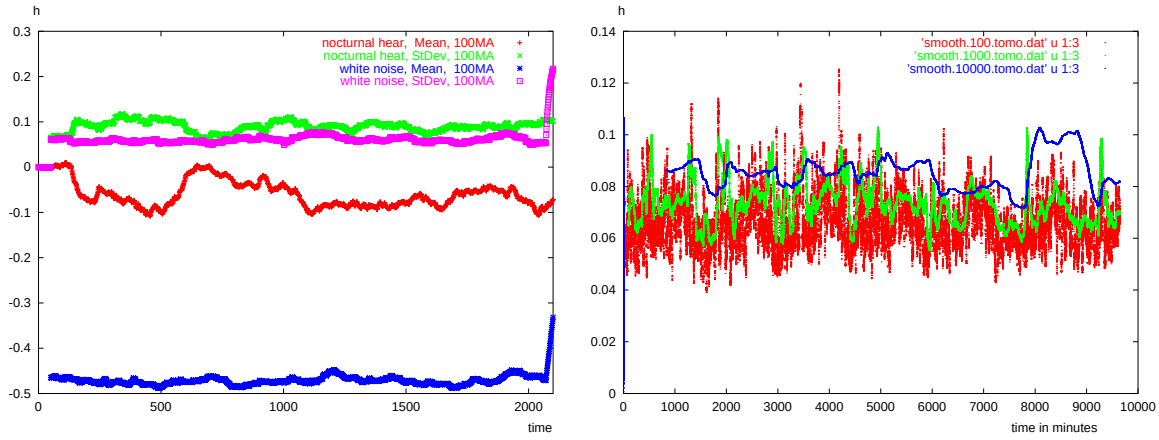


Figure 6: Left: Plot of the 100 base $MA$ smoothed effective Hölder exponent, for the heartbeat test case and for white noise. Mean and standard deviation are shown. Right: Three widths of $MA$ window, 100, 1000 and 10000 are used to test whether the fluctuations observed can be used to explain the wider multifractal spectra for the longer time series normally used for spectra estimation ($> 5000$ maxima).

*5.1 Ad. 1)*

We have included in the same plot, (figure 6 left), the result of running exactly the same procedure on a random noise sample and on the heartbeat rate. The resulting fluctuations for the random noise are much smaller in magnitude, thus supporting the observation that the fluctuations in variability of heartbeat may be of physiological or other origin and are not pure statistical fluctuations of noise data. Additionally, we checked the standard deviation of the variability, which clearly indicated a broader spectrum for the heartbeat than for the same length of white noise data.

'The reader may, of course, ask the question whether the non-stationarities in the Hölder exponent are the only source of wide multifractal spectrum of the heartbeat. Firstly, the non-stationarities observed show up at all temporal resolutions just as is the case for model multifractals. It is not possible to select one single temporal scale capturing the non-stationary behaviour. Therefore, the contributions to the multifractal spectrum come from various temporal scales in comparable degree.

If this were not the case, this would mean that for long base $MA$ averages, we would get considerably higher standard deviation of the Hölder exponent than for shorter base $MA$ averages.

Therefore, we performed a test to indicate whether the fluctuation effects observed can be used to explain the wider multifractal spectra. We used three widths of $MA$ window, 100, 1000 and 10000. The result of running $MA$ with the longest window (approximately 2 hours record) gave a clear indication that long lengths of data result in a wider spectra than shorter records. However, in defense of the multifractality of the heartbeat, we find in shorter base $MA$ levels of standard deviation which are larger than those in the longer base $MA$. In other words, locally, stdev (and therefore the 'local' multifractal spectrum) in $MA_{100}$ exceeds that of $MA_{1000}$. Similarly, locally stdev within a $MA_{1000}$ exceeds that of $MA_{10000}$. Note that it is *not* the plot in figure 6 b) that is being averaged. Rather, it gives the standard deviation of the result of averaging of the local effective Hölder exponent (not shown).

*5.2 Ad. 2)*

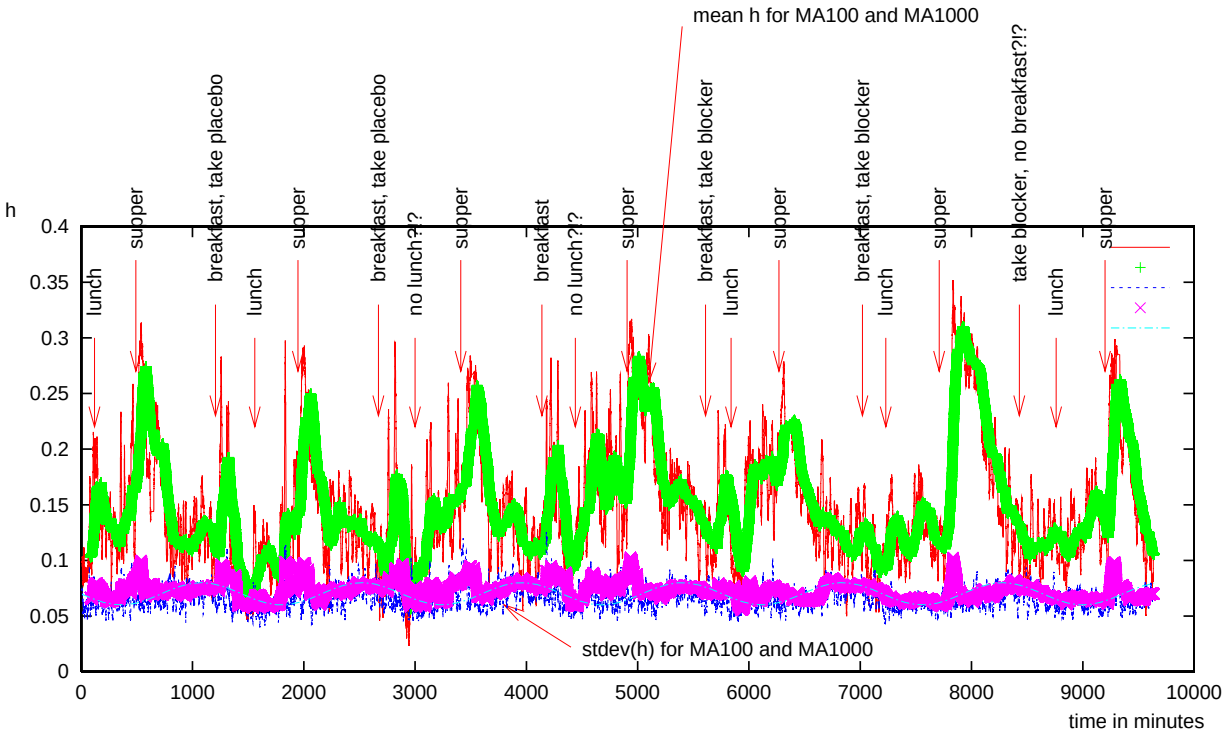


Figure 7: The variability plot from a long run of experiments where the test persons were given placebo or beta-blocker. Two runs of $MA$ filter were performed with 100 and 1000 maxima long window. The observed effect of the beta blocker is nihil or negligible. However, an interesting pattern of response to food is evident.

The variability plots shown in figures 7 and 8 come from a long run of experiments where the test persons were given placebo or beta-blocker. Two runs of $MA$ filter were performed with 100 and 1000 maxima long window. The observed effect of the beta blocker is nihil or negligible, indicating there is little change to the dynamics of the heart due to the beta-blocker only (at least for the two cases analysed and for the $s_{lo} = 5$ resolution considered). However, we found an interesting pattern of response to activity in these data sets. The first set shows a particularly strong response of the person in question to food. Let us remind the reader that higher values of the exponent are normally associated with a pathologic condition. The observed shift towards higher values as the result of

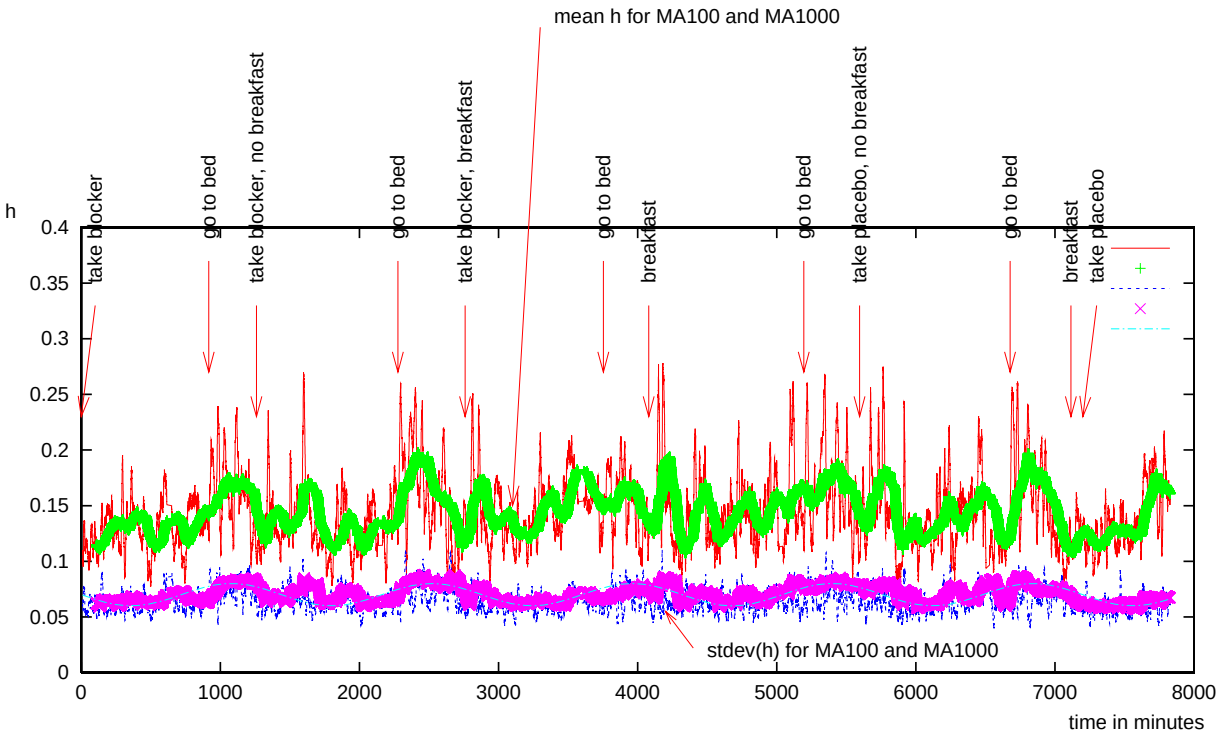


Figure 8: Another variability plot from with the placebo or beta-blocker. Again no response was registered. For this person, however, an interesting pattern of response to sleep has been found.

eating (it is almost possible to estimate the volume of the meal!) may indicate some nearly pathologic response in this individual case. Another data set shows a much smaller response to food but it does show higher correlation levels during first hours of sleep. Again this makes us speculate that the particular person may have nearly pathologic behaviour during first stages of sleep. (It should be noted that the person in study was going to bed very late 0am-2am and waking up after a relatively short sleep, 5-6 hours.)

*5.3 Ad. 3)*

Particularly in the second data set, the day/night oscillations [19] can be clearly observed in the width of the multifractal spectrum and the range of the variability (as is reflected by the standard deviation plotted in both figures 7 and 8). The oscillations nearly follow the sinusoidal line (with a 24 hour period), which we superimposed on the standard deviation of the local effective Hölder exponent. The actual phase of the oscillations is shifted by some 4-5 hours with respect to the clock. (It actually is 5-6 in the plot but about one hour delay comes from the $MA$ 1000 beat base average.) This means that the physiological 'middle of the night' is not at 12pm but at 4-6am, similarly 'middle of the day' falls at 4-6pm, not at 12noon.)

In the upper 'tomo.dat' plot in figure 9, the influence of the beta-blocker on the variability range (the width of the multifractal spectrum) can be observed. Especially during the day, standard deviation of the effective Hölder exponent is high, which would correspond with a wide multifractal spectrum calculated traditionally. This effect diminished after the placebo tablet was replaced with the beta-blocker. For the last three days of the test, the standard deviation of the Hölder exponent looks much smoother and seems to follow the day/night sinusoidal pattern better. This effect is not visible in the lower 'kou.dat' plot, where the beta-blocker was taken during the first few days of the test and was later replaced with placebo.

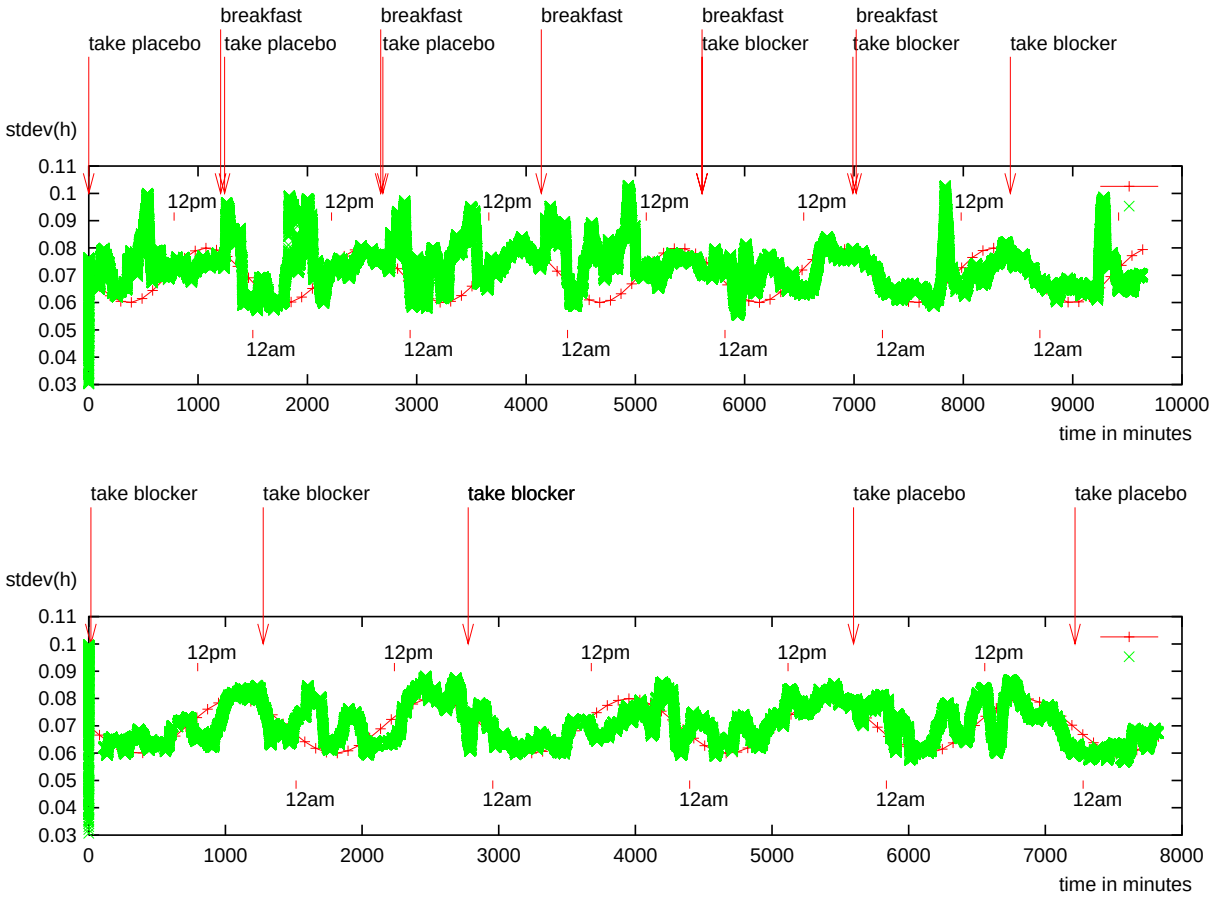


Figure 9: The day/night oscillations can be observed in the range of the variability as reflected by the standard deviation of the local effective Hölder exponent. The actual phase of the oscillations is shifted by some 4-6 hours with respect to the clock. (This means that the physiological 'middle of the night' is not at 12pm but at 4-6am, similarly the 'middle of the day' falls at 4-6pm, not at 12noon.) In the upper 'tomo.dat' plot, the influence of the beta-blocker on the variability range (the width of the Multifractal spectrum) can be observed. This is not visible in the lower 'kou.dat' plot.

*5.4 Ad. 4)*

In figure 10, two samples of the sleep period taken from the tomo and kou data are displayed. The actual time period between going to bed and waking up is indicated with a line segment. A part of the sinusoidal day/night rhythm is also visible, reaching maximum somewhere near the early morning hours (4-6am). The mean effective Hölder exponent obtained with 100 base $MA$ is shown together with the standard deviation from the mean. Both show large non-stationarities, different for each sample (and each night period within samples), but still considerably larger than statistical fluctuations would be in a monofractal (e.g. white) noise sample of comparable length.

The origin of these non-stationarities is not known at the moment of writing. It is possible that they are related to sleep phases [18], but this relation does not appear to be trivial and a follow-up study is expected to shed more light on this.

*5.5 Let us summarize*

We were able to test answers to the questions posed in the Introduction:

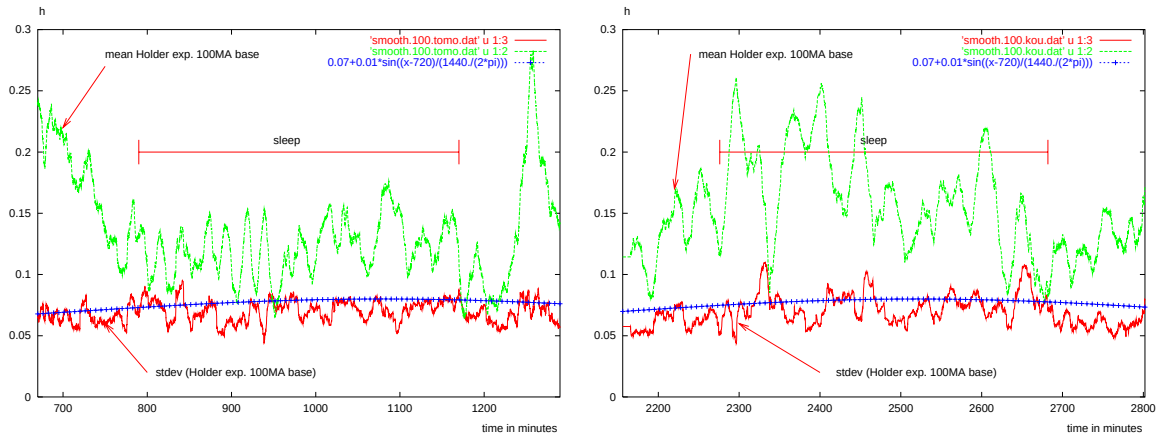


Figure 10: Two samples of the sleep period taken from the tomo and kou data. The time period between going to bed and waking up is indicated with a line segment. The mean effective Hölder exponent obtained with 100 base $MA$ is shown together with the standard deviation from the mean. Both show large non-stationarities. A part of the sinusoidal day/night rhythm is also visible.

1. The observed multifractal behaviour of the heartbeat is the result of 'non-stationarity' of the local effective Hölder exponent at all resolutions, just as is the case with multifractals. We still do not know the actual mechanism of these non-stationarities. Probably different mechanisms control them at various temporal resolutions.

2. Yes, for particular temporal resolutions (we tested about 100-1000 maxima), it is evident that the non-stationarity can be linked with activity. The exact mechanism of this dependence must be further studied since it cannot be validated from a limited test of the kind presented here.

3. It seems that the influence of beta-blocker is rather small and limited mainly to the standard deviation of the Hölder exponent (corresponding with the width of the multifractal spectra). In the only case where we observed such a dependence, it was narrowing the spectra width (less 'dynamic' behaviour) due to the beta blocker. The beta blocker does not seem to influence the mean value of the Hölder exponent (which reflects the correlation properties of the heartbeat).

4. We observe a full range of non-stationary behaviour in the case of non-activity such as during sleep; it seems to be mainly non-stationarity of shorter time scales.

Finally, we note that the local information revealed with the effective Hölder exponent seems to have potential diagnostic meaning. In particular this holds for fluctuations revealed with the $MA$ procedure. Their link with activity may be interesting to explore further in a diagnostic context. Of course, the global properties like the log-histogram, which can be calculated from the effective Hölder exponent, inherit the diagnostic capabilities of the MF spectra calculated traditionally [1]. In addition to this, it seems possible to display the mapping

$$h_{MA_n}(i) \rightarrow SDh_{MA_n}(i) \ ,$$

between the mean and the standard deviation for the investigated signals. The non-stationarities and their interrelation will be captured in such a map. Below we plotted it for two test signals tomo and kou for two resolutions $MA_{100}$. and $MA_{1000}$. The ranges, shape and compactness (or the degree of scatter) of these plots clearly differ for both records, which makes us guess that they may have diagnostic meaning.

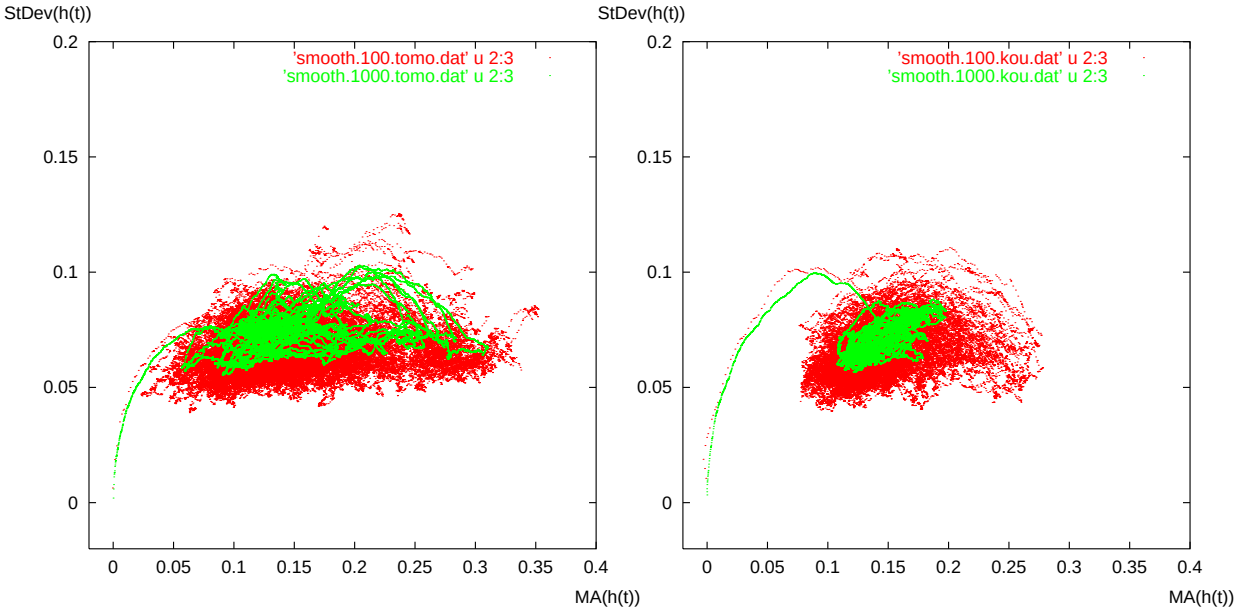


Figure 11: stdev versus mean maps for kou.dat and tomo.dat. 100 and 1000 $MA$ bases are plotted with different colours. The ranges, shape and compactness (or the degree of scatter) of these plots clearly differ for both records and may have diagnostic meaning. (Line going to 0.0 is due to finite sample size.) Note that both characteristics are not of the input signal but its local effective Hölder exponent and, therefore, can be compared without normalising. Due to the very fine dot size, the local dot density in these maps can be readily perceived. In general, binning the dots may be required, especially for longer time series records.

## 6. Conclusions

The local effective Hölder exponent has been applied to evaluate variability of heart rate locally at an arbitrary position (time) and resolution (scale). The variability so obtained is compatible in the sense of distribution to the multifractal spectra of the analysed heart rate time series. This provides the possibility to standardize the variability estimation for comparison between different patients and between different recordings for one patient.

In addition to this, we observed intriguing patterns on non-stationary behaviour of the local effective Hölder exponent. These can be related to individual response in variability records to daily activities.

We have attempted to build a methodological approach aiming at revealing such non-stationarities in local variablity at various time scales. A moving average filtering of Hölder exponent based variability estimates was used to enhance these fluctuations/non-stationarities.

We find that this way of local presentation of scaling properties may be of clinical importance. But, ultimately, we believe that the findings and methodology presented open a way better to address the question of physiological reasons for apparent multifractal behaviour of the heartbeat.

## Acknowledgments

The author would like to thank Plamen Ivanov for discussions, especially in the context of $MA$ filtering of the Hölder exponent. Help with the heartbeat data [17] is also greatly appreciated.
Thanks to Gene Stanley for encouraging the colour panels idea, in particular in the blind tests.
Special thanks go to Yoshi Yamamoto for kindly providing long records of heartbeat.
Arno Siebes, thanks for supporting this work.
This work has been carried out with the financial support from the Impact project.

# References


1. P.Ch. Ivanov, M.G. Rosenblum, L.A. Nunes Amaral, Z.R. Struzik, S. Havlin, A.L. Goldberger and H.E. Stanley, Multifractality in Human Heartbeat Dynamics. *Nature* **399**, (1999).
2. C.-K. Peng, J. Mietus, J.M. Hausdorff, S. Havlin, H.E. Stanley and A.L. Goldberger Long-Range Anticorrelations and Non-Gaussian Bahavior of the Heartbeat *Phys. Rev. Lett.*, vol. 70, p. 1343-1346, 1993.
3. A. Arneodo, E. Bacry and J.F. Muzy, Wavelets and Multifractal Formalism for Singular Signals: Application to Turbulence Data. *PRL*, **67**, No 25, 3515 (1991).
4. A. Arneodo, E. Bacry and J.F. Muzy, The Thermodynamics of Fractals Revisited with Wavelets. *Physica A*, **213**, 232 (1995).
   J.F. Muzy, E. Bacry and A. Arneodo, The Multifractal Formalism Revisited with Wavelets. *Int. J. of Bifurcation and Chaos* **4**, No 2, 245 (1994).
5. A. Arneodo, A. Argoul, J.F. Muzy, M. Tabard and E. Bacry, Beyond Classical Multifractal Analysis using Wavelets: Uncovering a Multiplicative Process Hidden in the Geometrical Complexity of Diffusion Limited Aggregates. *Fractals* **1**, 629 (1995).
6. A. Arneodo, E. Bacry, P.V. Graves and J.F. Muzy, Characterizing Long-Range Correlations in DNA Sequences from Wavelet Analysis. *PRL*, **74**, No 16, 3293 (1995).
7. P.Ch. Ivanov, M.G. Rosenblum, C.-K. Peng, J. Mietus, S. Havlin, H.E. Stanley and A.L. Goldberger, Scaling Behaviour of Heartbeat Intervals Obtained by Wavelet-based Time-series Analysis. *Nature*, **383**, 323 (1996).
8. Z. R. Struzik, Local Effective Hölder Exponent Estimation on the Wavelet Transform Maxima Tree, in *Fractals: Theory and Applications in Engineering*, Eds: M. Dekking, J. Lévy Véhel, E. Lutton, C. Tricot, Springer Verlag, (1999).
9. Z. R. Struzik, Determining Local Singularity Strengths and Their Spectra with the Wavelet Transform, to appear in *Fractals*, Vol 8, No 2, June 2000.
10. Z.R. Struzik The Wavelet Transform in the Solution to the Inverse Fractal Problem. *Fractals* **3** No.2, 329 (1995).
    Z.R. Struzik, From Coastline Length to Inverse Fractal Problem: The Concept of Fractal Metrology. *Thesis*, University of Amsterdam. (1996). Z.R. Struzik,
11. I. Daubechies, *Ten Lectures on Wavelets*, (S.I.A.M., 1992).

12. M. Holschneider, *Wavelets - An Analysis Tool*, (Oxford Science Publications, 1995).
13. S.G. Mallat and W.L. Hwang, Singularity Detection and Processing with Wavelets. *IEEE Trans. on Information Theory* **38**, 617 (1992).
14. S.G. Mallat and S. Zhong Complete Signal Representation with Multiscale Edges. *IEEE Trans. PAMI* **14**, 710 (1992).
15. S. Jaffard, *Multifractal Formalism for Functions: I. Results Valid for all Functions, II. Self-Similar Functions*, SIAM J. Math. Anal., 28(4): 944-998, 1997.
16. A. Arneodo, E. Bacry and J.F. Muzy, Solving the Inverse Fractal Problem from Wavelet Analysis, *Europhysics Letters*, **25**, No 7, 479–484, (1994).
17. http://www.physionet.org/physiobank
18. T. Penzel, A. Bunde, J. Heitmann, J.W. Kantelhardt, J.H. Peter, K. Voigt, Sleep-Stage-Dependent Heart Rate Variability in Patients with Obstructive Sleep Apnea. In: *Computers in Cardiology*, Vol. 26: 249-252. 1999.
19. P. Ch. Ivanov, A. Bunde, L. A. N. Amaral, J. Fritsch-Yelle, R. M. Baevsky, S. Havlin, H. E. Stanley, and A. L. Goldberger, Sleep-wake Differences in Scaling Behavior of the Human Heartbeat: Analysis of Terrestrial and Long-term Space Flight Data, *Europhys. Lett.* **48**, 594-600 (1999).